CD14 MODULATES PI3K/AKT/p38-MAPK "LICENSING" OF NEGATIVE REGULATORS OF TLR SIGNALING TO RESTRAIN CHRONIC INFLAMMATION

Bikash Sahay[1], Rebeca L. Patsey[1], Nicole Whatley[1], Sasmita Nayak[1,2], Christian H. Eggers[3,4], Justin D. Radolf[5,6], and Timothy J. Sellati[1*]

[1]Center for Immunology and Microbial Disease, Albany Medical College, Albany, NY 12208

[2]Present address: Department of Biology, Rensselaer Polytechnic Institute, Troy, NY 12180

[3]Department of Medicine, University of Connecticut Health Center, Farmington, CT 06030

[4]Present address: Department of Biomedical Sciences, Quinnipiac University, Hamden, CT 06518

[5]Departments of Medicine and [6]Genetics and Developmental Biology, University of Connecticut Health Center, Farmington, CT 06030

Correspondence should be addressed to Dr. Timothy J. Sellati, Center for Immunology and Microbial Disease, Albany Medical College, 47 New Scotland Avenue, MC151, ME205B, Albany, NY 12208-3479. Telephone: (518) 262-8140, Fax: (518) 262-2885, E-mail address: sellatt@mail.amc.edu

Nonstandard abbreviations used: MEMs, microbe expressed structural molecules; MOI, multiplicity of infection; p.i., post-infection; qRT-PCR, quantitative real-time PCR.

Key words: Bacterial, Monocytes/macrophages, Cell Surface Molecules, Signal Transduction

ABSTRACT

Current thinking emphasizes the primacy of CD14 in facilitating TLR recognition of microbes to initiate proinflammatory signaling events and the importance of p38-MAPK in augmenting such responses. Herein, this paradigm is challenged by demonstrating that recognition of *Borrelia burgdorferi* not only triggers an inflammatory response in the absence of CD14, but one that is uncontrolled as a consequence of impaired PI3K/AKT/p38-MAPK signaling and negative regulation of TLR2. CD14 deficiency results in hyperphosphorylation of AKT and reduced activation of p38. Such aberrant signaling leads to decreased negative regulation by SOCS1, SOCS3, and CIS thereby engendering a more severe and persistent inflammatory response to *B. burgdorferi*. Perturbation of this CD14/p38-MAPK-dependent mechanism of immune regulation may underlie development of infectious chronic inflammatory syndromes.

Toll-like receptor (TLR) signaling orchestrates innate response to the microbe-expressed molecular structures (MEMS) associated with pathogens. The principal proinflammatory MEMS of the human spirochetal pathogen *Borrelia burgdorferi*, the causative agent of Lyme disease, are triacylated lipoproteins recognized by heterodimers of TLR2 and TLR1[1]. Such recognition by TLR2 activates the NF-κB, MAPK, and PI3K/AKT pathways which coordinately regulate inflammation-associated gene activities responsible for host defense[2]. Although many aspects of Lyme disease pathogenesis remain ill-defined, it generally is accepted that clinical manifestations result primarily, perhaps entirely, from the host's local immune response to spirochetes[3].

CD14, a GPI-anchored protein expressed by macrophages (MΦ) and neutrophils, facilitates TLR-dependent proinflammatory cytokine production. Mice deficient for CD14 and their MΦ exhibit hyporesponsiveness when exposed to MEMS in the form of a bacterial lysate or purified agonists such as LPS, lipoproteins, and their synthetic analogs[4-6]. This hyporesponsiveness has been attributed to (i) the lower affinity of non-CD14-complexed LPS for TLR4[7], (ii) the requirement for CD14 in MyD88-independent signaling[8], and/or (iii) the inability of p38, a member of the serine/threonine MAPK family, to be induced in the absence of CD14[9]. Reviewing the literature one might conclude that CD14 is indispensable for elaboration of an inflammatory response to its cognate MEMs[4-6]. Surprisingly, however, both *in vitro* and *in vivo* recognition of several pathogens (e.g., *Borrelia burgdorferi, Staphylococcus aureus, Salmonella typhimurium,* and *Streptococcus* or *Klebsiella pneumoniae*) in the absence of CD14 leads to exaggerated proinflammatory cytokine production and worsening disease[10-13].

Following exposure of host cells to pathogens or their isolated constituents, p38 is activated through phosphorylation[14]. The action of p38 drives maturation of the phagosome following microbial uptake[15], activates downstream kinases that result in the translocation of NF-κB[16], stabilizes mRNA encoding cytokines[17], and activates genes encoding suppressors of cytokine signaling 3 (SOCS3) which negatively regulates pathogen-induced inflammation[18]. Because the pleiotropic action of p38 is thought to augment inflammation, the pharmaceutical industry has actively pursued development of potent and specific p38 inhibitors for the treatment of various inflammatory disorders[14]. However, it has been reported that inhibition of p38 both *in vitro* and *in vivo* results in higher cytokine production and more severe disease in a mouse model

of pneumococcal pneumonia and tuberculosis[19]. More recently, inhibition of p38 has been linked with sustained expression of TNF receptor-1, which perpetuates TNF-α induced NF-κB signaling[20].

Herein we advance a mechanistic explanation for these dichotomous findings which distinguishes CD14-dependent from -independent signaling and recognition of live *B. burgdorferi* versus lysed spirochetes. Using a murine model of Lyme borreliosis we show that CD14 deficiency results in (i) dysregulation of the PI3K/AKT/p38-MAPK pathway, (ii) loss of negative regulation of TLR2 signaling, (iii) increased cytokine production, and (iv) inefficient clearance of bacteria by MΦ. *In vitro* studies of cytokine response of $CD14^{+/+}$ and $CD14^{-/-}$ cells to live spirochetes reveal that inhibition of p38 augments the TNF-α response, and ablates the response to lysed organisms. Collectively, our results support the rather provocative notion that CD14 signaling is essential for prolonged p38 activation and thus clearance of bacteria as well as resolution of inflammation. Importantly therapeutic benefit derived from p38 inhibition in certain models of inflammation (e.g., rheumatoid arthritis)[14] may potentiate inflammatory processes under other circumstances (e.g. Lyme arthritis).

RESULTS

CD14 deficiency augments TLR-dependent gene activity. *B. burgdorferi*-induced activation of $CD14^{-/-}$ MΦ results in greater transcription, persistent surface expression of TLR2, and a concomitant increase in proinflammatory cytokine production, particularly TNF-α, compared to $CD14^{+/+}$ cells[12]. To more broadly evaluate the impact of CD14 deficiency on the inflammatory transcriptome of MΦ, we measured transcription of 84 genes associated with TLR signaling. Compared to cells expressing CD14, greater transcription of interleukins (i.e., IL-1α, IL-1β, IL-2, IL-6, IL-12, IFN-γ), chemokines (i.e., CCL-2), growth factors (i.e., G-CSF), and proinflammatory lipid mediators (i.e., COX2) was observed in $CD14^{-/-}$ MΦ at 24 h p.i. (**Fig 1a**). TLR2 transcript levels, but not those of other TLRs, were elevated 50-fold in $CD14^{-/-}$ MΦ compared to wild-type cells. Also, much of the dysregulated gene activity in the former cells was associated with the NF-κB signaling pathway. In $CD14^{+/+}$ MΦ gene induction peaked at 3 h and returned to baseline by 24 h p.i; in contrast, general gene activity was greater in $CD14^{-/-}$ cells at 3 h and remained elevated throughout the course of the experiment (data not shown) suggesting a critical role for CD14 in downmodulation of inflammatory signaling.

***B. burgdorferi* fails to trigger the expression of negative regulators of TLR signaling in the absence of CD14**. Negative regulators of TLR signaling include soluble (s) molecules (e.g., sMyD88 and sTLRs), competitive inhibitors (e.g., IRAKM), protein phosphatases [e.g., MAPK phosphatase 1, (MKP1)], E3 ligases (e.g., SOCSs), etc.[21]. The above findings prompted an evaluation of the impact of CD14 deficiency on several of these negative regulators. *B. burgdorferi* induced significantly higher transcription of *socs1* (~3.5-fold) in $CD14^{+/+}$ MΦ than in their $CD14^{-/-}$ counterparts by 6 h p.i. ($P < 0.05$) (**Fig. 1b**). Similarly, increased expression of SOCS-1 protein was observed in $CD14^{+/+}$ MΦ, whereas no expression was detected in their CD14-deficient counterparts (**Fig. 1c**). *Socs3* transcription also was greater in $CD14^{+/+}$ MΦ compared to $CD14^{-/-}$ cells (~3.5-fold at three h and ~2.5-fold at six h) ($P < 0.01$) (**Fig. 1b**). Owing to rapid proteosome-mediated degradation of SOCS3, this molecule only can be detected by Western blot analysis with addition of the proteosome inhibitor,

MG132 (10 μM), for one h prior to collection of MΦ co-incubated with *B. burgdorferi* for the specified time periods. Under these conditions, SOCS3 expression peaked in $CD14^{+/+}$ cells at six h whereas no expression was detected in MΦ lacking CD14 (**Fig. 1c**). $CD14^{+/+}$ cells also exhibited *cis* gene activity ~5.6-fold above that seen in $CD14^{-/-}$ MΦ ($P > 0.01$) (**Fig. 1b**). At its peak, *cis* transcript levels in wild-type cells were ~400-fold over mock controls. By 24 h p.i. transcription of these negative regulators in $CD14^{+/+}$ and $CD14^{-/-}$ MΦ was indistinguishable and transcription of *mkp1* and *irakm* was not significantly different in these cells at any time point studied (**Supplementary Fig 1**, online). Thus negative regulation of TLR signaling depends, at least in part, on CD14.

CD14 signaling regulates the activation state of IRF and STAT molecules. To elucidate why transcription of *socs1* and *socs3* is diminished in $CD14^{-/-}$ cells, we examined the expression of three transcription factors known to either directly or indirectly regulate their transcription[22, 23]. *B. burgdorferi* induced ~13-fold higher transcription of *irf1* in $CD14^{+/+}$ MΦ than in unstimulated controls ($P < 0.05$) (**Fig. 2a**). Transcription of both *irf7* and *stat1* was significantly higher in $CD14^{-/-}$ MΦ than in wild-type cells at 24 h (**Fig 2a**), whereas no differences were seen for *irf3, stat3,* or *stat4* (**Supplementary Fig 1**, online). Additionally, Western blot analysis revealed that phospho-STAT1, but not phospho-STAT3, levels were higher in $CD14^{+/+}$ than in $CD14^{-/-}$ MΦ (**Fig. 2b**). Diminished SOCS expression in $CD14^{-/-}$ MΦ is consistent with the observed reduction in transcriptional activation of *irf1* and STAT1 phosphorylation.

The inflammatory response to *B. burgdorferi* is perpetuated in the absence of CD14. The mouse model of Lyme borreliosis was used to elucidate the relationship between CD14 signaling, SOCS activity, and disease progression. Arthritis, an inflammatory hallmark of Lyme disease, is a self-limiting process in mice that peaks between 2 and 3 weeks p.i. and typically resolves by 6 weeks[24]. As previously reported for tick-mediated infection[12], syringe inoculation of mice with *B. burgdorferi* resulted in tibiotarsal joint swelling (reflective of synovitis/arthritis with periarticular edema) in $CD14^{+/+}$ and $CD14^{-/-}$ mice which peaked at 2 weeks p.i.. Contrary to $CD14^{-/-}$ joints, joint inflammation in the wild-type mice resolved by 3 weeks p.i. (**Fig. 3a**).

Beginning at 2 weeks p.i. and continuing for the duration of the experiment, the joints of $CD14^{-/-}$ mice were significantly more inflamed (P >0.001). Consistent with more severe and prolonged joint inflammation in $CD14^{-/-}$ mice (**Fig. 3a)**, transcription of *socs1* and *socs3* in joint tissue was greatly reduced compared to wild-type mice (**Fig. 3b**), as was the transcription of *cis* and *irakM* (data not shown).

One might predict a superior capacity to clear spirochetes in *B. burgdorferi*-infected $CD14^{-/-}$ mice by virtue of greater cytokine production (e.g., TNF-α and IFN-γ) (**Fig 7 and ref 12**). Surprisingly, all organs recovered from $CD14^{-/-}$ mice, with the exception of the heart, had heavier bacterial burdens than those of wild-type animals (**Fig. 3c**). Taken together, these data suggest an indispensable role for CD14-dependent signaling in negative regulation of inflammation, clearance of bacteria, and disease resolution.

Killing, but not internalization, of *B. burgdorferi* by MΦ is significantly impaired in the absence of CD14. A report that CD14 acts as a unique phagocytic receptor for Gram-negative bacteria[25] suggests this molecule may serve a similar function in spirochetal uptake. In light of the inverse relationship between expression of CD14 and spirochetal burden in infected tissues, we examined the impact of CD14 deficiency on phagocytosis *B. burgdorferi*. GFP-expressing spirochetes were internalized as readily by $CD14^{-/-}$ MΦ as by those expressing CD14 (**Fig. 4a**). Furthermore, neither the kinetics of internalization (**Fig. 4b**), nor the number of bacteria associated per cell, as measured by changes in mean fluorescence intensity, was influenced by CD14 deficiency (data not shown).

Killing of bacteria within the phagolysosomal compartment depends, at least in part, on the production of RNS/ROS[26]. Although differences in uptake were not observed, the ultimate fate of *B. burgdorferi* internalized by $CD14^{+/+}$ and $CD14^{-/-}$ MΦ might differ. Indeed, assessing gene activity both *in vitro* and *in vivo* it was observed that *inos* transcript levels were significantly higher in the cells from and the joints of $CD14^{+/+}$ mice (**Fig. 4c**). These differences were reflected in two-fold more cultivable spirochetes being recovered from 6 h-infected $CD14^{-/-}$ (7,252 bacteria/ml) versus $CD14^{+/+}$ (3,567 bacteria/ml) MΦ as measured using a modified tissue culture infective dose method.

CD14 signaling regulates activation of the p38-MAPK pathway, inhibition of which leads to lower SOCS3 and higher cytokine production by MΦ. A p38-STAT1-IRF1 signaling axis negatively regulates TLR2 activity while positively regulating iNOS, SOCS1, and SOCS3 activity[27]. To determine whether CD14 signaling modulates this axis, the phosphorylation state of p38 was evaluated in $CD14^{-/-}$ MΦ. In contrast to cells expressing CD14, detectable levels of phospho-p38 were only observed transiently in *B. burgdorferi*-stimulated $CD14^{-/-}$ MΦ (**Fig. 5a**). This result was confirmed and extended through use of a phospho-CBA kit; as seen in **Fig. 5b**, spirochetes stimulated CD14-dependent increases in the level of phospho-p38 in both a time- and dose-dependent manner. In contrast, no such changes were observed in the phosphorylation state of two other members of the MAPK family, ERK and JNK. Finally, it should be appreciated that given the known transcriptional inhibition of *tlr2* by p38[27], the higher transcription of this gene seen in **Fig. 1a** and expression of TLR2 on $CD14^{-/-}$ peritoneal MΦ is entirely consistent with the decreased phospho-p38 levels observed in $CD14^{-/-}$ MΦ (**Fig. 5a, 5b**).

Pharmacological inhibition of p38 has implicated this molecule in proinflammatory responses to a variety of stimuli of microbial, host, and environmental origin[14]. Thus, the coexistence of higher phospho-p38 and lower cytokine production by *B. burgdorferi*-stimulated $CD14^{+/+}$ MΦ was counterintuitive. To clarify the role of p38 in our model arctigenin, a general MAPK inhibitor, and SB202190, a p38-specific inhibitor, were used. These inhibitors significantly lowered the transcription of *socs3* and *inos* by $CD14^{+/+}$ MΦ in reponse to *B. burgdorferi* (**Fig. 5c**). As predicted based upon lower *socs3* transcript levels, arctigenin and SB202190 relieved the inhibition of TNF-α release by wild-type cells (**Fig. 5d**) and did so in a dose-dependent fashion (**Supplementary Fig 2**, online). In stark contrast, SB203580 decreased TNF-α production by cells co-incubated with borrelial lysate (10 μg/ml), (**Fig. 5e**). This latter finding is entirely consistent with the widely-reported observation that p38 enhances cellular inflammatory responses to isolated bacterial MEMS[16, 28] and underscores the difference between stimulation of cells with live spirochetes as opposed to spirochetal lysates or lipoproteins[12, 16, 29, 30].

Suppression of the PI3K/AKT axis reimposes regulation of proinflammatory cytokine production by CD14$^{-/-}$ MΦ. Detection of phospho-p38 for only a brief period implied strict CD14-dependent modulation of this signaling cascade (**Fig. 5a**). p38-MAPK is negatively regulated through activation of AKT, a serine-threonine kinase activated via PI3K[31]. The levels of phospho-AKT in CD14$^{-/-}$ MΦ were significantly increased above baseline and above that seen in cells expressing CD14 (**Fig. 6a**). Of note, peak phosphorylation of AKT in CD14-/- cells appeared to immediately precede disappearance of phospho-p38 (**Fig. 5a**, 10 min). The PI3K inhibitors wortmannin and Ly294002 were used, to determine whether AKT activity contributing to decreased phospho-p38 levels. As shown in Fig. 6B, exposure of cells to either inhibitor for 30 min prior to incubation with *B. burgdorferi* eliminated the phospho-AKT pool (**Fig. 6b**). Blocking PI3K-dependent AKT function should result in de-repression of p38 phosphorylation[31]. Ly294002, but not wortmannin, treatment of CD14$^{-/-}$ MΦ resulted in a further ~2-fold enhancement of p38 phosphorylation (**Fig. 6b**) following co-incubation with *B. burgdorferi*. The inability of wortmannin to have the same effect as Ly294002 may be attributable to its known "off target" inhibition of the p38-MAPK pathway[32]. To explore further how signaling through the PI3K/AKT axis influences *B. burgdorferi*-induced MΦ activation, spirochetes were incubated with CD14$^{-/-}$ cells that were untreated or treated with Ly294002. Enhanced phosphorylation of p38 correlates with a profound reduction in *B. burgdorferi*-induced TNF-α secretion by CD14$^{-/-}$ MΦ whereas nearly 10-fold more TNF-α is secreted in the absence of the inhibitor (**Fig. 6c**), an effect that is dose-dependent (**Supplementary Fig. 3,** online).

In the absence of CD14, *B. burgdorferi* triggers TNF-α production in both a TLR2-dependent and -independent fashion. Recognition that *B. burgdorferi* stimulates innate host responses primarily through engagement of TLR2[33, 34] led us to consider whether the uncontrolled release of TNF-α by CD14$^{-/-}$ MΦ correlates with their dramatically increased expression of TLR2 (**Fig. 1a** and **Ref. 12**). To answer this question, mice deficient for CD14 or TLR2 (each backcrossed 10 generations onto a C3H/HeN background) were crossed to establish animals homozygous recessive for both loci. MΦ expressing CD14 and TLR2 and those deficient for individual or both loci were co-incubated with *B. burgdorferi* and TNF-α levels were measured (**Fig 7**). In

the absence of CD14, TNF-α production was significantly higher compared to their wild-type counterparts at 24 hp.i.. TLR2 deficiency had the opposite effect insofar as TNF-α release was significantly reduced compared to wild-type MΦ at 6 h and 24 h p.i.. Remarkably, the cell's capacity to secrete TNF-α in the absence of both CD14 and TLR2 was partially or fully restored to the levels released by $CD14^{-/-}$ and wild-type MΦ, respectively. This finding is very significant as it demonstrates that, despite similarities in the exaggerated Lyme disease phenotype observed in $CD14^{-/-}$ and $TLR2^{-/-}$ mice, these two signaling pathways are not entirely synonymous.

DISCUSSION

Regulation of the host response to *B. burgdorferi* begins with CD14 recognition of lipoproteins[12, 35]. In the absence of such receptor engagement, Lyme borreliosis is typified by greater bacterial burden, more severe histopathology, and dysregulated production of proinflammatory immunomodulators[12]. Given that binding of borrelial lipoproteins to CD14 facilitates downstream signaling through TLR2 and the cytosolic adaptor protein MyD88 it is perhaps not surprising that mice deficient for these molecules also harbor more bacteria in their tissues and present with more severe arthritis[36-38]. Despite similar pathophysiological features in *B. burgdorferi*-infected mice lacking CD14, TLR2, or MyD88, CD14 is distinct in its ability to tightly regulate cytokine production both *in vitro* and *in vivo*[12]. CD14's unique role as an anti-inflammatory receptor is supported further by the observation that signaling in its absence increases production of proinflammatory cytokines in response to infection with *Staphylococcus aureus*[10]. A similar trend towards greater cytokine production in response to *E. coli* bioparticles was seen with $CD14^{-/-}$ versus $CD14^{+/+}$ peritoneal MΦ[39]. Finally, blockade of CD14 by monoclonal antibody treatment increased tissue invasion and resulted in higher TNF-α production in rabbits infected with *Shigella flexneri*[40].

Coordinate signaling through CD14 and TLR2 simultaneously activates NF-κB, p38-MAPK, and PI3K pathways[2, 41] to orchestrate both the initiation and resolution of inflammatory responses to *B. burgdorferi*. CD14 deficiency, however, leads to excessive phosphorylation of AKT along with higher transcription and surface expression of TLR2[12]. Given that TLR2 signaling regulates PI3K activity and leads to AKT activation, we were led to consider that either elevated TLR2 expression and/or higher phospho-AKT levels in $CD14^{-/-}$ MΦ underlie the more severe and persistent course of Lyme borreliosis in these mice. Cytokine release by *B. burgdorferi*-activated MΦ deficient for both CD14 and TLR2 was comparable to that of wild-type cells, but was significantly greater than that observed with $TLR2^{-/-}$ cells and less than that of $CD14^{-/-}$ cells. This finding suggests only a partial role for TLR2 in recognition of *B burgdorferi*, one that is strictly proinflammatory, and implies the existence of another receptor(s) for bacterial recognition in the absence of CD14.

One candidate non-TLR receptor is complement receptor 3 (CR3), a member of the β2-integrin family of adhesion molecules[42]. Using CHO cells transfected with CD14, TLR2, and CR3 in various combinations it

was revealed that the "inside-out" signaling responsible for increasing the avidity of CR3 for its ligand requires both CD14 and TLR2[43]. Similarly, antibodies directed against CD14 and/or TLR2 were shown to block "inside-out" signaling required for CR3-mediated recognition of *Porphyromonas gingivalis* fimbriae[44]. Moore and coworkers reported that inhibition of CR3 signaling reduced by 50% the *E. coli*-stimulated secretion of TNF-α by $CD14^{-/-}$ peritoneal MΦ[39]. These various studies also implicate CR3 in uptake of bacteria[39, 43, 44]. Like CD14, this phagocytic receptor resides within the lipid raft and clustering of CR3 precedes PI3K-mediated phosphorylation and activation of AKT[42]. In light of the ability of CR3 to mediate internalization of *B burgdorferi* (personal communication, Juan Anguita, Veterinary & Animal Sciences, University of Massachussetts, Amherst) and its capacity to activate PI3K, it is intriguing to speculate on whether CR3 is a phagocytic receptor in the absence of CD14 whose action may account for higher cytokine production during infection. Such a role is supported by the fact that spirochetal uptake was not diminished in the absence of CD14.

AKT has pleiotropic effects that include promotion of cell survival, NF-κB activation, and inhibition of ASK1, a MAPKKK responsible for p38 activity[31, 45]. p38 activity is associated with NF-κB activation and stabilization of mRNA encoding proinflammatory cytokines such as TNF-α[17]. That inhibition of PI3K prevented phosphorylation of AKT and thus increased p38 activity in *B. burgdorferi*-activated $CD14^{-/-}$ MΦ is consistent with the inverse relationship between AKT and p38 activity. Unexpectedly, however, PI3K inhibition also resulted in decreased TNF-α production, a finding inconsistent with higher p38 activity and its accepted role as a proinflammatory mediator[14]. Nevertheless, inhibition of p38 in $CD14^{+/+}$ cells with either general or specific antagonists resulted in lower *inos* and *socs3* transcription and a dose-dependent increase in TNF-α production in response to *B. burgdorferi*. Contrarily, it has been reported that SB203580 inhibits TNF-α release by the mouse macrophage RAW264.7 cell line in response to borrelial lysates[16]. One potential explanation for these divergent findings is that the "context" in which bacterial MEMS are recognized (i.e., live spirochetes versus lysed organisms) influences the downstream signaling cascades initiated within the host cell. Consistent with this idea, treatment of $CD14^{+/+}$ MΦ with SB203580 inhibited TNF-α production in response to borrelial lysates as previously reported[16]. This suggests that, in conjunction with CD14 and TLR2 engagement,

phagocytic receptors with a differential capacity to internalize live spirochetes versus a lysate may orchestrate intracellular signaling events, a notion supported by earlier studies[12, 29]. The anti-inflammatory capacity of p38 is further demonstrated in mouse models of pneumococcal pneumonia and tuberculosis where its inhibition results in impaired bacterial clearance and increased TNF-α production both *in vitro* and *in vivo*[19]. It also has been established that p38 induces the shedding of TNF receptor-1 from activated cells thus dampening their responsiveness to TNF-α[20]. The combination of increased TNF-α production and maintenance of its cognate receptor on the cell surface likely contributes to the cytokine "surge" and exacerbates the pathology associated with bacterial infection. Taken together, these results challenge the notion that isolated MEMS (e.g., purified LPS, lipoproteins, etc.) are equivalent to the whole organisms from which they are extracted[12, 29]. They also sound a cautionary note regarding application of p38 inhibitors to treat inflammatory disorders especially those of infectious-origin. Development of immunotherapeutic strategies that enhance the action of SOCS may represent a more fruitful avenue in pursuit of novel anti-inflammatory drugs[46-48].

Finally, another set of intriguing observations was the persistent arthritis and increased spirochetal-burden in the tissues of $CD14^{-/-}$ mice. Considering the importance of bacterial clearance as an element of disease resolution, we evaluated CD14 as a potential phagocytic receptor for spirochetes. Consistent with the findings of Moore et al. using *E. coli* bioparticles[39], we report that CD14 deficiency does not impair internalization of spirochetes. During the process of engulfment various receptors are engaged which initiate kinase and phosphatase cascades that facilitate killing of phagocytosed bacteria. Despite the equivalent capacity of $CD14^{+/+}$ and $CD14^{-/-}$ MΦ to engulf spirochetes, activation of p38 in the $CD14^{-/-}$ cells was transient and thus insufficient, either *in vitro* or *in vivo*, to drive the transcription of *inos* and *irf1* whose gene products participate in maturation of the phagosome and bacterial killing[49]. The lower transcript levels of *inos* in $CD14^{-/-}$ MΦ likely are associated with decreased RNS/ROS production[50] and may contribute, at least in part, to the higher bacterial burden observed in the infected tissues of these mice. In contrast to the association of IRF1 with early maturation of the phagosome, IRF7 induction occurs later in this process and often is linked to persistence of exogenous material within the phagosomal compartment, particularly in plasmacytoid dendritic cells (pDCs)[51]. Higher *irf7* transcription is a hallmark of activated pDCs and is necessary for the induction of

Type I IFN, an important element of viral and bacterial clearance[52]. Specifically, at a point when the *ifnβ* locus is transcriptionally silent in *B. burgdorferi*-activated CD14$^{-/-}$ MΦ little IRF7 mRNA is being transcribed. However, like activated pDCs, later in their activation program *irf7* transcription is significantly greater in CD14$^{-/-}$ cells than their wild-type counterparts. As in activated pDCs and RAW264.7 cells, where increased IRF7 coincides with an accumulation of viral antigen or purified TLR agonist (i.e., CpG ODNs)[51], we propose that "frustrated" clearance of borrelial antigen from the phagosomal compartment of CD14$^{-/-}$ MΦ may drive the transcription of *irf7*. A corollary of this scenario is that persistence of borrelial TLR agonists in the phagosomal compartment may perpetuate inflammatory signaling through TLR2 and other receptors of TLR or non-TLR origin.

In toto, we detail a critical and unanticipated role for CD14 in downmodulating TLR2-dependent and -independent pathways which regulate NF-κB signaling events. CD14 exerts its influence on the intensity and duration of inflammation through the PI3K/AKT/p38-MAPK axis which we propose serves as a "rheostat" to provide fine regulation of NF-κB activity, the "backbone" of the host's inflammatory response to pathogenic challenge. As depicted in our model (**Fig 8**), *B. burgdorferi*-initiated inflammatory signaling in the absence of CD14 stimulates greater AKT activity which enhances NF-κB signaling while at the same time suppressing p38 and STAT1. p38 and STAT1 are responsible for inducing IRF1 and SOCS activity which ultimately facilitates spirochete clearance and/or dampens cytokine production. Thus the more severe and persistent Lyme disease phenotype observed in CD14$^{-/-}$ mice reflects the concomitant increase in NF-κB-mediated proinflammatory signaling and loss of negative regulation via diminished SOCS activity. To our knowledge this is the first report implicating the CD14/p38-MAPK pathway as the driving force behind anti-inflammatory responses in a mouse model of bacterial infection.

METHODS

Reagents. Great care was taken during the preparation of all buffers and reagents to minimize contamination with environmental LPS by utilizing baked (180ºC for 4 h) and autoclaved glassware, disposable plasticware, and pyrogen-free H_2O that also is free of DNAse and RNAse activity.

Cultivation of *B. burgdorferi.* Low-passage *B. burgdorferi* strain 297 were maintained at 23°C in Barbour-Stoenner-Kelley medium containing 6% normal rabbit serum ($BSK_{complete}$) from Pel-Freez Biologicals (Rogers, AR) and then temperature-shifted to 37°C. Increased expression of OspC was confirmed by silver staining of whole borrelial lysates separated by SDS-PAGE. *B. burgdorferi* 297 expressing green fluorescent protein were cultivated in $BSK_{complete}$ containing 400 μg/ml kanamycin and were grown at 37°C until mid- to late-logarithmic phase for subsequent use in phagocytosis experiments as previously described[29].

Mice and infection protocol. Four to eight week-old C3H/HeN ($CD14^{+/+}$) mice (Taconic, Germantown, NY) were housed in the Animal Resources Facility at Albany Medical College. Food and water were provided *ad libitum* and all animal procedures conformed to the Institutional Animal Care and Use Committee guidelines. $CD14^{-/-}$ mice were generated as previously described[4] and subsequently backcrossed 10 generations onto a C3H/HeN background[12]. $TLR2^{-/-}$ mice were provided by Tularik Inc. (now Amgen Inc., South San Francisco, CA) and generated by Deltagen Inc. (Menlo Park, CA)[53] and were backcrossed 10 generations onto a C3H/HeN background. C3H/HeN mice deficient for CD14 and TLR2 were crossed to establish animals homozygous recessive for both alleles.

Mice were infected via intradermal administration of 5×10^5 spirochetes over the sternum. $BSK_{complete}$ was used as a mock-infection control. At one week intervals, tibiotarsal joint thickness was measured using digital calipers and bacterial burden in infected tissues was determined using isolated genomic DNA as previously described[12]. Total RNA also was isolated from infected tissues for qRT-PCR as described below.

Isolation and differentiation of MΦ. MΦ were isolated from the bone marrow of six to eight week-old mice. Briefly, bone marrow cells recovered by flushing femurs and tibia with DMEM were incubated in tissue culture-treated 25cm^2-flasks (BD Falcon, BD Biosciences, San Jose, CA) overnight at 37°C with 5% CO_2 to eliminate adherent fibroblasts, granulocytes, and any contaminating MΦ[54]. The following day, 1×10^7 suspension cells were maintained in 10-cm^2 bacteriological Petri dishes (BD-Falcon) for three days with DMEM supplemented with 10% fetal bovine serum, 20% L292-cell conditioned media, 0.01% HEPES, 0.01% sodium pyruvate, and 0.01% L-glutamine. Cultures were supplemented with five ml of the above-described medium and seven days after isolation cell monolayers were recovered using ice-cold PBS and scraping. Single cell suspensions were used immediately or frozen in liquid nitrogen with 20% FBS and 10% DMSO for use in future experiments.

***B. burgdorferi*-MΦ co-incubation.** MΦ were seeded into 6-well tissue culture-treated plates at a concentration of 1×10^6 cells/2 ml/well and allowed to adhere overnight. The following day, *B. burgdorferi* were enumerated and re-suspended as described above. MΦ were washed twice with serum-free DMEM to remove any traces of FBS and spirochetes (resuspended in DMEM + 4% autologous serum) were added at an MOI of 10 and co-incubated for different time intervals at 37°C in 5% CO_2. Cells incubated with DMEM + 4% autologous serum alone served as mock-infected controls.

Analysis of bacterial association with MΦ: *Fluorescence microscopic analysis.* MΦ were seeded into 8-well chamber slides (Lab-Tek™ II CC2 Chamber Slide™ System) at a concentration of 1×10^5 cells/200µl/well and allowed to adhere overnight. The following day, GFP-expressing *B. burgdorferi* were enumerated and added to cell monolayers at an MOI of 10 and co-incubated for different time intervals. After co-incubation, cells were washed twice with serum-free DMEM and were fixed with 4% paraformaldehyde for 30 min. GFP-expressing *B. burgdorferi* were visualized by fluorescence microscopy (Olympus UIS2Series: U-MNG2 Green excitation mirror unit/NIB HIGHQ FITC). *Flow cytometric analysis.* MΦ were aliquoted into five ml polystyrene round-bottom tubes (BD Biosciences, Bedford, MA) at a concentration of 5×10^5 cells/600µl/tube, centrifuged at 250

× *g* for 10 min followed by incubation with GFP-expressing *B. burgdorferi* resuspended in DMEM + 4% autologous serum at an MOI of 10. Cells and bacteria were coincubated for different time intervals, washed twice in FA buffer (BD Microbiological Systems, Sparks, MD) and fixed in FA buffer containing 4% paraformaldehyde. Sample data was acquired on a BD FACSCanto^{TM} Flow Cytometer (BD Immunocytometry Systems) and results were analyzed using FlowJo software (Ashland, OR).

Quantitative real-time PCR. Total RNA was isolated from MΦ using the RNeasy Mini Kit (Qiagen GmbH, Hilden, Germany) as per the manufacturer. The amount and purity of RNA was quantified by Biophotometer (Eppendorf AG, Hamburg, Germany) and 0.5µg were used for reverse transcription of cDNA using Superscript II (Invitrogen Corporation, CA, USA). cDNA (20µl) served as the template in quantitative real-time PCR (qrt-PCR) analysis using Mouse TLR Signaling Pathway RT^2 Profiler™ PCR Arrays (Superarray Bioscience). These arrays contain primer pairs for 84 genes implicated in TLR signal transduction as well as housekeeping genes and controls in a 96-well microtiter plate format. This qrt-PCR methodology directly quantifies transcript levels based upon the $2^{-\Delta\Delta Ct}$ method through measurement of SYBR green fluorescence using an iQ5 real-time PCR detection system (Bio-Rad Laboratories, Hercules, CA).

For transcriptional analysis of genes not represented on the RT^2 Profiler™ PCR Array, qrt-PCR was performed in a final volume of 25µl containing: 12.5µl of 2X SYBR green master mix (Bio-Rad Laboratories), 25pMol of the specific forward and reverse primers, and 0.2µl of cDNA. Primers were designed using Beacon Designer version 7.0 software (PREMIER Biosoft Intl, Palo Alto, CA) and the sequences of specific primer sets are provided in **Supplemental Table 1** online. Amplification conditions were 95°C (3 min) and 40 cycles of 95°C (15s), 55°C (40s) and 72°C (30s). All the qrt-PCR reactions were run in triplicate with no-template controls (NTC) and mean c*T* values were used for all the calculations using 18S rRNA as an internal control for normalization. Effects greater than a two-fold change with respect to mock control were considered significant.

Western blot analysis. Antibodies directed against SOCS1, SOCS3 and CIS were obtained from Santa Cruz Biotechnology, Inc. (Santa Cruz, CA), antibodies against AKT, STAT1, STAT3 and p38 were obtained from

Cell Signaling Technology, Inc. (Danvers, MA), and antibodies against β-actin were obtained from Bethyl Laboratories, Inc. (Montgomery, TX). Protein samples (25-100μg, depending on the target) were resolved by SDS-PAGE and transferred to nitrocellulose using semi-dry transblot (Bio-Rad Laboratories, Hercules, CA). The membrane was blocked with 5% non-fat milk and then incubated overnight at 4°C with primary antibody (1:1000, for AKT and STATs; 1:100 for SOCS; and 1:10,000 for β-actin). Membranes were probed with HRP-conjugated anti-rabbit IgG (Cell Signaling Technology) diluted 1:2000. Specific signal was developed using the SuperSignal West-Dura chemiluminescent substrate (Pierce Endogen, Rockford, IL) and recorded either on photographic film or using a FluorChem 7700 Chemiluminescence Imager (Alpha Innotech, San Leandro, CA).

Cytometric bead array (CBA) for cytokine and phospho-protein analysis. MΦ were co-incubated with *B. burgdorferi* at various MOI and cytokine levels were measured in the recovered culture supernatant using the Mouse Inflammation CBA kit and a FACSArray flow cytometer [BD Immunocytometry Systems (BDIS), San Jose, CA]. Data was acquired and analyzed using BD FACSArray software and FCAP Array software, version 1.0 (BDIS), respectively. For phospho-protein analysis, the protein content of the samples was normalized, added to a phospho-specific CBA kit, and analyzed as described above.

Inhibition of signaling cascades by pharmacological inhibitors. MΦ were treated with the inhibitors arctigenin (1μM), SB202190 (0.5μM), SB203580 (10μM), wortmannin (100nM), and Ly294002 (100μM) for 30 min prior to addition of *B. burgdorferi*. In some experiments a range of inhibitor concentrations was used. DMSO alone served as a control. Culture supernatants were collected for cytokine measurement and cells were lysed for RNA isolation and Western blot analysis.

Statistical analysis. All results were expressed as mean ± SEM and comparisons between the groups were made using one-way ANOVA followed by Bonferroni's correction. Differences between control and experimental groups were considered significant using $\alpha = 0.05$.

ACKNOWLEDGMENTS

We thank Drs. James Drake, Jonathan Harton, Karsten Hazlett (Albany Medical College, NY), and Juan Anguita (University of Massachusetts, Amherst, MA) for critical review of the manuscript. Special thanks to Aaloki Shah and Sally Catlett (Albany Medical College, NY) for technical support and Daniel Desrosiers (University of Connecticut Health Science Center, CT) for computer graphic design. Supported by the National Institutes of Health (AI054546 to TJS; AI29735 and AI38894 to JDR) and an Arthritis Foundation Investigator Award to TJS.

AUTHOR CONTRIBUTIONS

B.S. designed the study, did and analyzed experiments and contributed to manuscript preparation; R.L.P., N. W. and S. N. did and analyzed experiments; C.H.E. generated the GFP-expressing *B. burgdorferi*; J.D.R. provided GFP-expressing *B. burgdorferi* and contributed to manuscript preparation; T.J.S. designed and organized the study and contributed to manuscript preparation.

FIGURE LEGENDS

Figure 1. Higher *B. burgdorferi*-induced inflammatory gene activity is associated with lower SOCS levels in $CD14^{-/-}$ MΦ. Total RNA from $CD14^{+/+}$ and $CD14^{-/-}$ MΦ co-incubated with *B. burgdorferi* was analyzed by qrt-PCR (**a**) for genes involved in the TLR signaling pathway or (**b**) for *socs1*, *socs3*, and *cis*. Results presented in (**a**) reflect the ratio of fold changes in HPRT-normalized gene activity in $CD14^{-/-}$ versus $CD14^{+/+}$ MΦ. All results represent mean ± SEM. $*P < 0.05$, $** P < 0.01$. (**c**) Equivalent protein amounts of lysed MΦ were separated by 12% SDS-PAGE, transferred to a PVDF membrane and probed with antibodies directed against SOCS1, SOCS3, CIS, or β-actin.

Figure 2. IRF1, IRF7 and STAT1 are differentially activated by *B. burgdorferi* in the absence of CD14. (a) Total RNA from $CD14^{+/+}$ and $CD14^{-/-}$ MΦ co-incubated with *B. burgdorferi* was analyzed by qrt-PCR for *irf1, irf7 and stat1*. Results represent mean ± SEM. $*P < 0.05$, $** P < 0.01$. (**b**) Equivalent protein amounts of lysed MΦ were separated by 12% SDS-PAGE, transferred to a nitrocellulose membrane and probed with phospho-specific STAT1 or STAT3, or β-actin antibodies.

Figure 3. Reduced *socs* transcription is associated with impaired bacterial clearance and more severe and prolonged Lyme arthritis. (**a**) $CD14^{+/+}$ and $CD14^{-/-}$ mice were infected with 5×10^5 *B. burgdorferi*, and tibiotarsal joint thickness was measured at 1-wk intervals. The horizontal bars indicate mean thickness for each group and the data are representative of two independent experiments (n=24). (**b**) Total RNA was isolated from the tibiotarsal joints of $CD14^{+/+}$ and $CD14^{-/-}$ mice (n=6) and an equal amount of RNA was pooled from each joint and 0.5 μg was used for preparing cDNA. The cDNA was analyzed by qRT-PCR to determine the *in vivo* levels of *socs1* and *socs3* transcription. Data are representative of two independent experiments. (**c**) Organs were collected six weeks p.i. and DNA was isolated for quantification of bacterial burden. Results represent mean ± SEM. $*P < 0.05$, $** P < 0.01$, $*** P < 0.001$.

Figure 4. *B. burgdorferi*-induced transcription of *inos*, but not phagocytic uptake of spirochetes, is impaired by CD14 deficiency. GFP-expressing *B. burgdorferi* were co-incubated with $CD14^{+/+}$ and $CD14^{-/-}$ MΦ for the indicated times and phagocytosis was evaluated by (**a**) fluorescence microscopy and (**b**) flow cytometry. (**c**) *inos* transcript levels were determined by qrt-PCR using RNA isolated from MΦ co-incubated with *B. burgdorferi* or using RNA pooled from joints isolated from infected mice as described in the legend for **Fig. 3**. Results represent mean ± SEM. *$P < 0.05$, ** $P < 0.01$, *** $P < 0.001$.

Figure 5. CD14 deficiency results in dysregulated p38-MAPK signaling and cytokine production in response to *B. burgdorferi.* (**a**) Equivalent protein amounts of lysed $CD14^{+/+}$ and $CD14^{-/-}$ MΦ co-incubated with *B. burgdorferi* were separated by SDS-PAGE, transferred to a nitrocellulose membrane and probed with phopho-p38 and β-actin antibodies. (**b**) MΦ were co-incubated with *B. burgdorferi* at different MOI and equal amounts of total protein were used to estimate relative phosphorylated MAPK levels by phospho-specific CBA. The data shown are representative of two independent experiments. (**c**) $CD14^{+/+}$ MΦ were treated with DMSO alone, SB202190 (0.5 μM), or arctigenin (1 μM), for 30 min prior to co-incubation with *B. burgdorferi* at an MOI of 10 and total RNA was analyzed by qrt-PCR for *inos* and *socs3*. (**d**) $CD14^{+/+}$ MΦ were treated as described in (**c**), and culture supernatants were analyzed for the presence of TNF-α by CBA. (**e**) $CD14^{+/+}$ MΦ were treated with DMSO alone or increasing concentrations of SB203580 for 30 min prior to co-incubation with *B. burgdorferi* lysate (10μg/ml). Cell-culture supernatants were collected and TNF-α levels were measured by CBA. Results in (c-e) represent mean ± SEM. *$P < 0.05$, ** $P < 0.01$, *** $P < 0.001$.

Figure 6. Inhibition of *B. burgdorferi*-induced AKT activation in $CD14^{-/-}$ MΦ reestablishes p38 activity and restores negative regulation of cytokine production. (**a**) Equivalent protein amounts of lysed $CD14^{+/+}$ and $CD14^{-/-}$ MΦ co-incubated with *B. burgdorferi* were separated by SDS-PAGE, transferred to a nitrocellulose membrane and probed for phospho-AKT and β-actin. The blot shown is representative of two independent experiments. (**b**) $CD14^{-/-}$ MΦ were treated with DMSO alone or PI3K inhibitors [wortmannin (100nM) or

Ly294002 (100μM)] for 30 min prior to co-incubation with *B. burgdorferi.* Western blots of cellular protein were probed with phospho-specific AKT and p38 antibodies and then striped and reprobed for total AKT, p38, and β-actin. The data shown are representative of two independent experiments. (**c**) $CD14^{+/+}$ and $CD14^{-/-}$ MΦ were treated with Ly294002 (100μM) for 30 min prior to co-incubated with *B. burgdorferi* for three and six h. Culture supernatants were collected and TNF-α levels were measured by CBA. Results represent mean ± SEM. *** $P < 0.001$.

Figure 7. TLR2 plays a partial role in CD14-independent cytokine production. MΦ isolated from $CD14^{+/+}$, $CD14^{-/-}$, $TLR2^{-/-}$and $CD14^{-/-}/TR2^{-/-}$ mice were co-incubated with *B. burgdorferi* for the indicated time points, cell culture supernatants were collected and TNF-α was measured by CBA. Results represent mean ± SEM. *** $P < 0.001$.

Figure 8. Proposed model for CD14-dependent and -independent signaling in response to infection with *B. burgdorferi*. In the absence of CD14, greater activation of AKT inhibits p38 activity resulting in increased transcription of TLR2, reduced activation of STAT1 and IRF1, and decreased induction of SOCS necessary to modulate the intensity and duration of Lyme borreliosis. The size of the red circles indicates relative phosphorylation status of the indicated protein and the size of the individual protein(s) is reflective of relative transcript/protein levels.

Supplementary Figure 1. *mkp1*, *irakm irf3*, *stat3* and *stat4* transcription is CD14-independent and unaltered by its absence. Total RNA from $CD14^{+/+}$ and $CD14^{-/-}$ MΦ co-incubated with *B. burgdorferi* was analyzed by qrt-PCR for *mkp1*, *irakm, irf3*, *stat3,* and *stat4*. Results represent mean ± SEM.

Supplementary Figure 2. Inhibition of p38 or MAPK results in a dose-dependent increase of TNF-α production in $CD14^{+/+}$ cells. $CD14^{+/+}$ MΦ were treated with DMSO or the indicated concentrations of arctigenin, SB202190 or SB203580 for 30 min prior to co-incubation with *B. burgdorferi*. Cell culture

supernatants were collected 24 h post incubation and TNF-α levels were measured by CBA. Results represent mean ± SEM. *** $P < 0.001$.

Supplementary Figure 3. Inhibition of PI3K results in a dose-dependent decrease in TNF-α production by $CD14^{-/-}$ cells. $CD14^{-/-}$ MΦ were treated with DMSO or the indicated concentration of LY294002 for 30 min prior to co-incubation with *B. burgdorferi*. Cell-culture supernatants were collected 24 h post incubation and TNF-α levels were measured by CBA. Results represent mean ± SEM. *** $P < 0.001$.

Supplementary Table 1. Primer sequences used in qrt-PCR

References

1. Wooten,R.M. & Weis,J.J. Host-pathogen interactions promoting inflammatory Lyme arthritis: use of mouse models for dissection of disease processes. *Curr. Opin. Microbiol.* **4**, 274-279 (2001).

2. Arbibe,L. *et al.* Toll-like receptor 2-mediated NF-[kappa]B activation requires a Rac1-dependent pathway. *Nat Immunol* **1**, 533-540 (2000).

3. Steere,A.C. & Glickstein,L. Elucidation of Lyme arthritis. *Nat Rev. Immunol* **4**, 143-152 (2004).

4. Haziot,A. *et al.* Resistance to endotoxin shock and reduced dissemination of gram-negative bacteria in CD14-deficient mice. *Immunity* **4**, 407-414 (1996).

5. Antal,S. Evaluation of CD14 in host defence. *European Journal of Clinical Investigation* **30**, 167-179 (2000).

6. Sellati,T.J. *et al.* Treponema pallidum and Borrelia burgdorferi lipoproteins and synthetic lipopeptides activate monocytic cells via a CD14-dependent pathway distinct from that used by lipopolysaccharide. *J Immunol* **160**, 5455-5464 (1998).

7. Landmann,R., Muller,B., & Zimmerli,W. CD14, new aspects of ligand and signal diversity. *Microbes. Infect.* **2**, 295-304 (2000).

8. Jiang,Z. *et al.* CD14 is required for MyD88-independent LPS signaling. *Nat Immunol* **6**, 565-570 (2005).

9. Han,J., Lee,J.D., Bibbs,L., & Ulevitch,R.J. A MAP kinase targeted by endotoxin and hyperosmolarity in mammalian cells. *Science* **265**, 808-811 (1994).

10. Haziot,A. *et al.* CD14 plays no major role in shock induced by Staphylococcus aureus but down-regulates TNF-alpha production. *J Immunol* **162**, 4801-4805 (1999).

11. Heumann,D., Lauener,R., & Ryffel,B. The dual role of LBP and CD14 in response to Gram-negative bacteria or Gram-negative compounds. *J Endotoxin. Res.* **9**, 381-384 (2003).

12. Benhnia,M.R. *et al.* Signaling through CD14 attenuates the inflammatory response to Borrelia burgdorferi, the agent of Lyme disease. *J Immunol* **174**, 1539-1548 (2005).

13. Echchannaoui,H. *et al.* CD14 deficiency leads to increased MIP-2 production, CXCR2 expression, neutrophil transmigration, and early death in pneumococcal infection. *J Leukoc Biol* **78**, 705-715 (2005).

14. Schieven,G.L. The biology of p38 kinase: a central role in inflammation. *Curr. Top. Med. Chem.* **5**, 921-928 (2005).

15. Blander,J.M. & Medzhitov,R. Regulation of phagosome maturation by signals from toll-like receptors. *Science* **304**, 1014-1018 (2004).

16. Olson,C.M. *et al.* p38 mitogen-activated protein kinase controls NF-kappaB transcriptional activation and tumor necrosis factor alpha production through RelA phosphorylation mediated by mitogen- and stress-activated protein kinase 1 in response to Borrelia burgdorferi antigens. *Infect. Immun.* **75**, 270-277 (2007).

17. Dean,J.L.E., Sully,G., Clark,A.R., & Saklatvala,J. The involvement of AU-rich element-binding proteins in p38 mitogen-activated protein kinase pathway-mediated mRNA stabilisation. *Cellular Signalling* **16**, 1113-1121 (2004).

18. Bode,J.G. *et al.* The MKK6/p38 mitogen-activated protein kinase pathway is capable of inducing SOCS3 gene expression and inhibits IL-6-induced transcription. *Biol Chem.* **382**, 1447-1453 (2001).

19. van den Blink,B. *et al.* p38 Mitogen-Activated Protein Kinase Inhibition Increases Cytokine Release by Macrophages In Vitro and During Infection In Vivo. *J Immunol* **166**, 582-587 (2001).

20. Ogura,H. *et al.* ERK and p38 MAP kinase are involved in downregulation of cell surface TNF receptor 1 induced by acetoxycycloheximide. *Int. Immunopharmacol.* **8**, 922-926 (2008).

21. Liew,F.Y., Xu,D., Brint,E.K., & O'Neill,L.A. Negative regulation of toll-like receptor-mediated immune responses. *Nat Rev Immunol* **5**, 446-458 (2005).

22. Saura,M., Zaragoza,C., Bao,C., McMillan,A., & Lowenstein,C.J. Interaction of interferon regulatory factor-1 and nuclear factor kappaB during activation of inducible nitric oxide synthase transcription. *J Mol Biol* **289**, 459-471 (1999).

23. Saito,H. *et al.* IFN regulatory factor-1-mediated transcriptional activation of mouse STAT-induced STAT inhibitor-1 gene promoter by IFN-gamma. *J Immunol* **164**, 5833-5843 (2000).

24. Moody,K.D. & Barthold,S.W. Lyme borreliosis in laboratory mice. *Lab Anim Sci* **48**, 168-171 (1998).

25. Schiff,D.E. *et al.* Phagocytosis of gram-negative bacteria by a unique CD14-dependent mechanism. *J. Leukocyte Biol.* **62**, 786-794 (1997).

26. Steinberg,B.E., Huynh,K.K., & Grinstein,S. Phagosomal acidification: measurement, manipulation and functional consequences. *Biochem Soc. Trans.* **35**, 1083-1087 (2007).

27. Li,J.D. Exploitation of host epithelial signaling networks by respiratory bacterial pathogens. *J Pharmacol. Sci.* **91**, 1-7 (2003).

28. Chen,G. *et al.* Bacterial endotoxin stimulates macrophages to release HMGB1 partly through. *J Leukoc Biol* **76**, 994-1001 (2004).

29. Moore,M.W. *et al.* Phagocytosis of Borrelia burgdorferi and Treponema pallidum Potentiates Innate Immune Activation and Induces Gamma Interferon Production. *Infect. Immun.* **75**, 2046-2062 (2007).

30. Cruz,A.R. *et al.* Phagocytosis of Borrelia burgdorferi, the Lyme Disease Spirochete, Potentiates Innate Immune Activation and Induces Apoptosis in Human Monocytes. *Infect. Immun.* **76**, 56-70 (2008).

31. Kim,A.H., Khursigara,G., Sun,X., Franke,T.F., & Chao,M.V. Akt Phosphorylates and Negatively Regulates Apoptosis Signal-Regulating Kinase 1. *Mol. Cell. Biol.* **21**, 893-901 (2001).

32. Ferby,I.M., Waga,I., Sakanaka,C., Kume,K., & Shimizu,T. Wortmannin inhibits mitogen-activated protein kinase activation induced by platelet-activating factor in guinea pig neutrophils. *J. Biol. Chem.* **269**, 30485-30488 (1994).

33. Wooten,R.M. *et al.* Toll-like receptor 2 plays a pivotal role in host defense and inflammatory response to Borrelia burgdorferi. *Vector. Borne. Zoonotic. Dis.* **2**, 275-278 (2002).

34. Lien,E. *et al.* Toll-like Receptor 2 Functions as a Pattern Recognition Receptor for Diverse Bacterial Products. *J. Biol. Chem.* **274**, 33419-33425 (1999).

35. Wooten,R.M. *et al.* The role of CD14 in signaling mediated by outer membrane lipoproteins of Borrelia burgdorferi. *J Immunol* **160**, 5485-5492 (1998).

36. Wooten,R.M. *et al.* Toll-Like Receptor 2 Is Required for Innate, But Not Acquired, Host Defense to Borrelia burgdorferi. *J Immunol* **168**, 348-355 (2002).

37. Liu,N., Montgomery,R.R., Barthold,S.W., & Bockenstedt,L.K. Myeloid differentiation antigen 88 deficiency impairs pathogen clearance but does not alter inflammation in Borrelia burgdorferi-infected mice. *Infect. Immun.* **72**, 3195-3203 (2004).

38. Bolz,D.D. *et al.* MyD88 plays a unique role in host defense but not arthritis development in Lyme disease. *J Immunol* **173**, 2003-2010 (2004).

39. Moore,K.J. *et al.* Divergent Response to LPS and Bacteria in CD14-Deficient Murine Macrophages. *J Immunol* **165**, 4272-4280 (2000).

40. Wenneras,C. *et al.* Blockade of CD14 increases Shigella-mediated invasion and tissue destruction. *J Immunol* **164**, 3214-3221 (2000).

41. Matsuzawa,A. *et al.* ROS-dependent activation of the TRAF6-ASK1-p38 pathway is selectively required for TLR4-mediated innate immunity. *Nat Immunol* **6**, 587-592 (2005).

42. Dib,K. BETA 2 integrin signaling in leukocytes. *Front Biosci.* **5**, D438-D451 (2000).

43. Sendide,K. *et al.* Cross-talk between CD14 and complement receptor 3 promotes phagocytosis of mycobacteria: regulation by phosphatidylinositol 3-kinase and cytohesin-1. *J Immunol* **174**, 4210-4219 (2005).

44. Hajishengallis,G., Shakhatreh,M.A., Wang,M., & Liang,S. Complement receptor 3 blockade promotes IL-12-Mediated Clearance of Porphyromonas gingivalis and Negates Its Virulence In Vivo. *J Immunol* **179**, 2359-2367 (2007).

45. Koyasu,S. The role of PI3K in immune cells. *Nat Immunol* **4**, 313-319 (2003).

46. Shouda,T. *et al.* Induction of the cytokine signal regulator SOCS3/CIS3 as a therapeutic strategy for treating inflammatory arthritis. *J Clin. Invest* **108**, 1781-1788 (2001).

47. Wong,P.K. *et al.* SOCS-3 negatively regulates innate and adaptive immune mechanisms in acute IL-1-dependent inflammatory arthritis. *J Clin. Invest* **116**, 1571-1581 (2006).

48. Egan,P.J., Lawlor,K.E., Alexander,W.S., & Wicks,I.P. Suppressor of cytokine signaling-1 regulates acute inflammatory arthritis and T cell activation. *J Clin. Invest* **111**, 915-924 (2003).

49. Blander,J.M. & Medzhitov,R. On regulation of phagosome maturation and antigen presentation. *Nat Immunol* **7**, 1029-1035 (2006).

50. Forman,H.J. & Torres,M. Redox signaling in macrophages. *Mol Aspects Med* **22**, 189-216 (2001).

51. Honda,K. *et al.* Spatiotemporal regulation of MyD88-IRF-7 signalling for robust type-I interferon induction. *Nature* **434**, 1035-1040 (2005).

52. Decker,T., Muller,M., & Stockinger,S. The Yin and Yang of type I interferon activity in bacterial infection. *Nat Rev Immunol* **5**, 675-687 (2005).

53. Werts,C. *et al.* Leptospiral lipopolysaccharide activates cells through a TLR2-dependent mechanism. *Nat Immunol* **2**, 346-352 (2001).

54. Warren,M.K. & Vogel,S.N. Bone marrow-derived macrophages: development and regulation of differentiation markers by colony-stimulating factor and interferons. *J Immunol* **134**, 982-989 (1985).

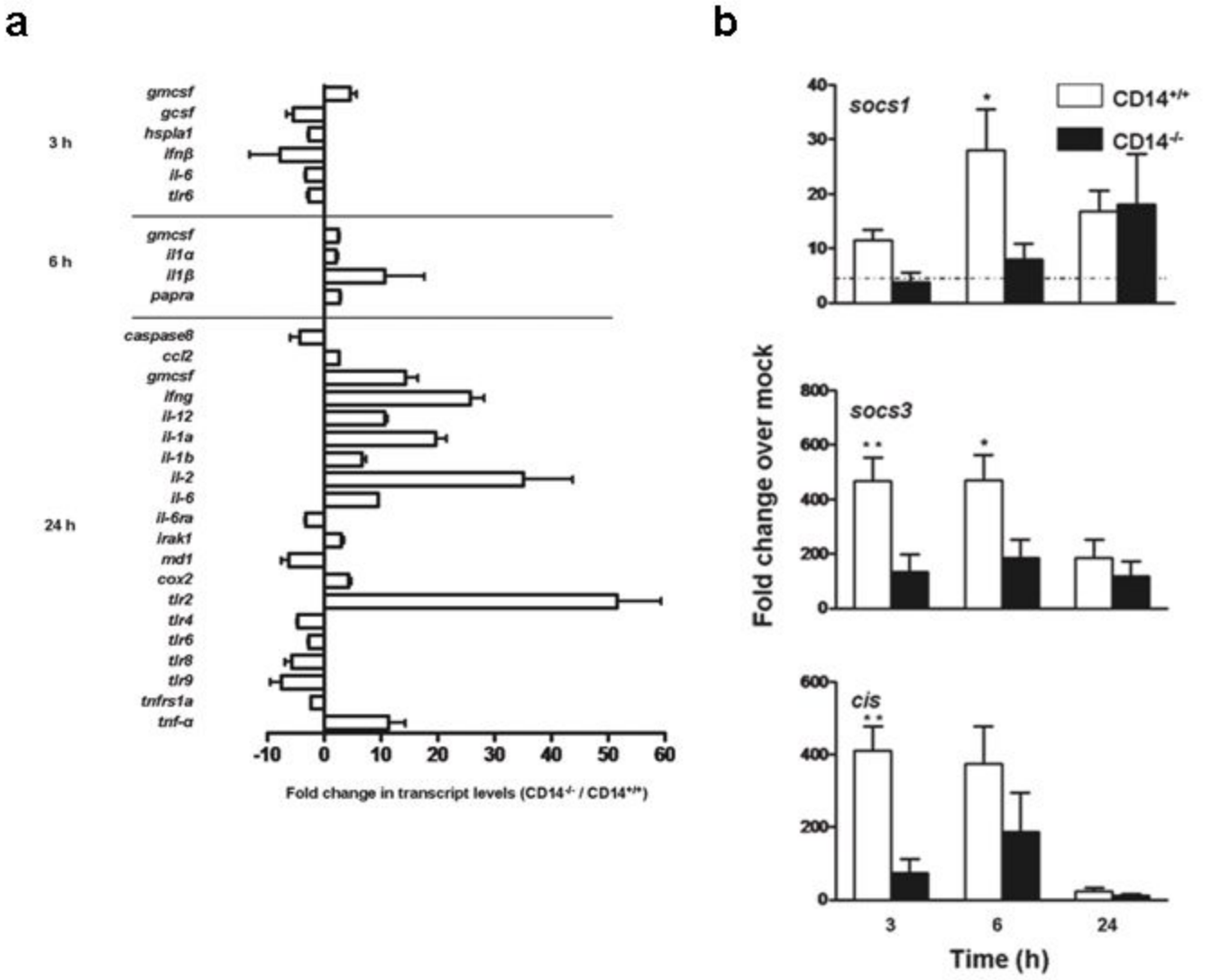
a
3 h
6 h
24 h
gmcsf
gcsf
hspla1
lfnβ
il-6
tlr6
gmcsf
il1α
il1β
papra
caspase8
ccl2
gmcsf
lfng
il-12
il-1a
il-1b
il-2
il-6
il-6ra
irak1
md1
cox2
tlr2
tlr4
tlr6
tlr8
tlr9
tnfrs1a
tnf-α
-10 0 10 20 30 40 50 60
Fold change in transcript levels (CD14-/- / CD14+/+)
b
socs1
CD14+/+
CD14-/-
socs3
cis
Fold change over mock
3 6 24
Time (h)
c
CD14+/+
CD14-/-
Time (h)
0 2 4 6 8 10 12
SOCS1
β-actin
CIS
β-actin
DMSO
MG132
B.b.
3 6 24
SOCS3
β-actin

a

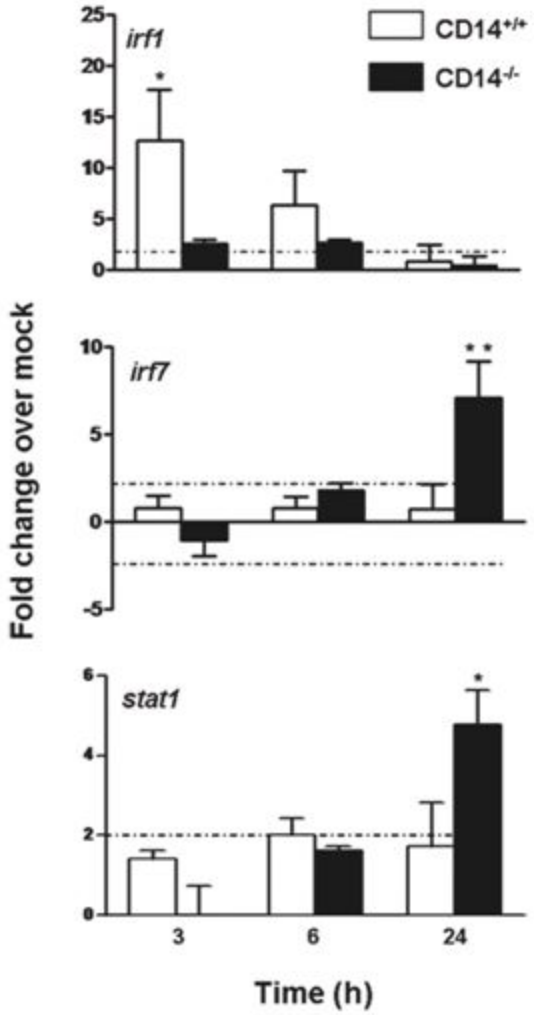
CD14+/+
CD14-/-
irf1
irf7
stat1
Fold change over mock
Time (h)
3
6
24

b

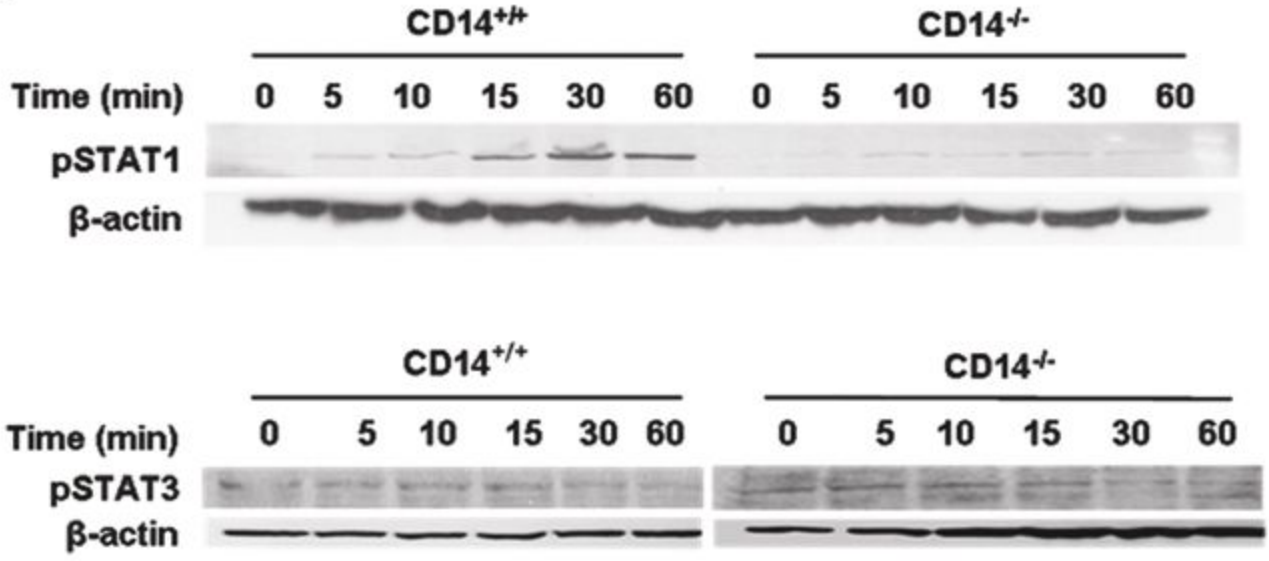
CD14+/+
CD14-/-
Time (min)
0 5 10 15 30 60
pSTAT1
β-actin
pSTAT3

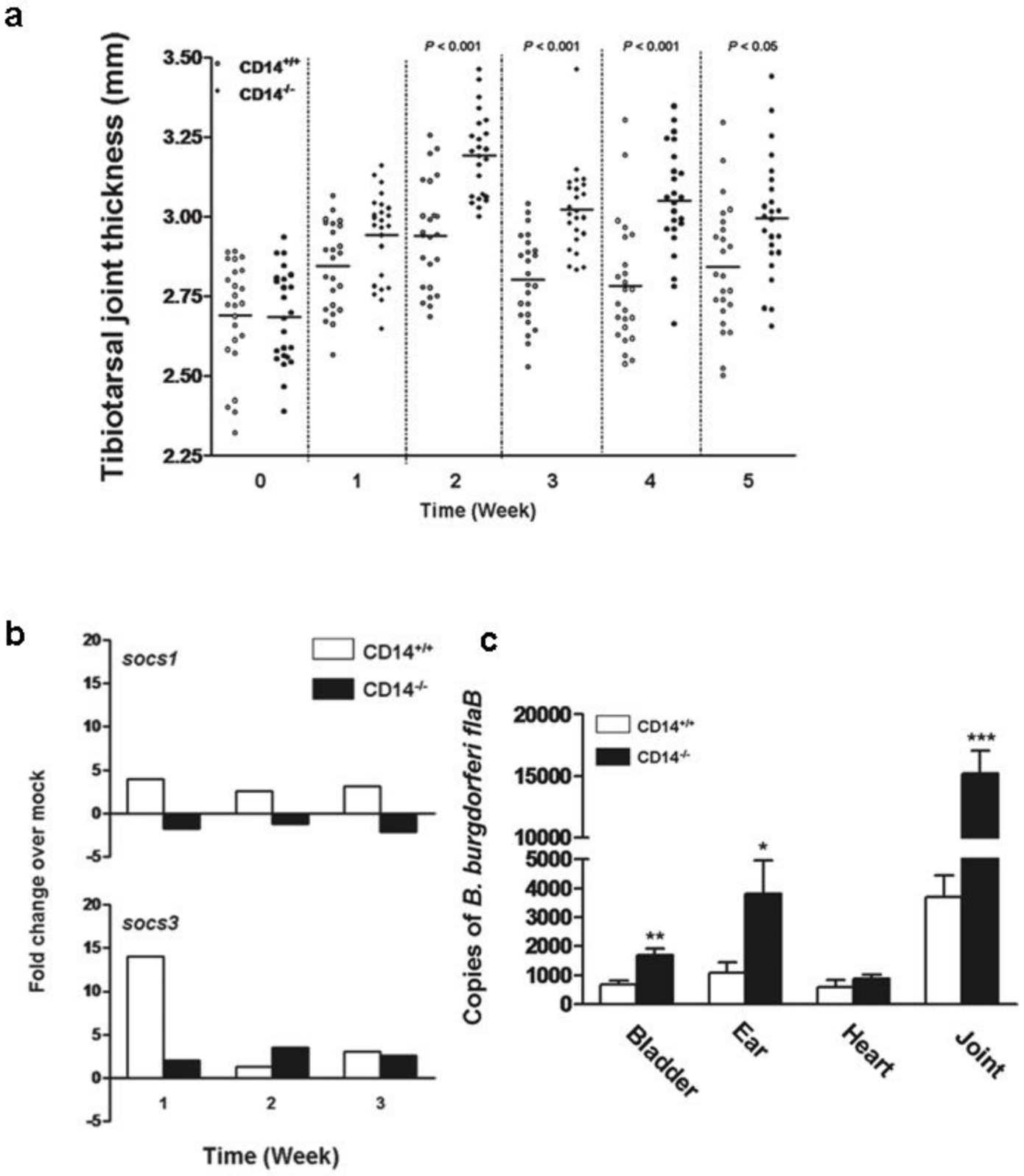
a
Tibiotarsal joint thickness (mm)
3.50
3.25
3.00
2.75
2.50
2.25
CD14+/+
CD14-/-
P < 0.001
P < 0.001
P < 0.001
P < 0.05
0
1
2
3
4
5
Time (Week)
b
socs1
socs3
CD14+/+
CD14-/-
Fold change over mock
20
15
10
5
0
-5
1
2
3
Time (Week)
c
Copies of B. burgdorferi flaB
20000
15000
10000
5000
4000
3000
2000
1000
0
CD14+/+
CD14-/-
**
*
***
Bladder
Ear
Heart
Joint

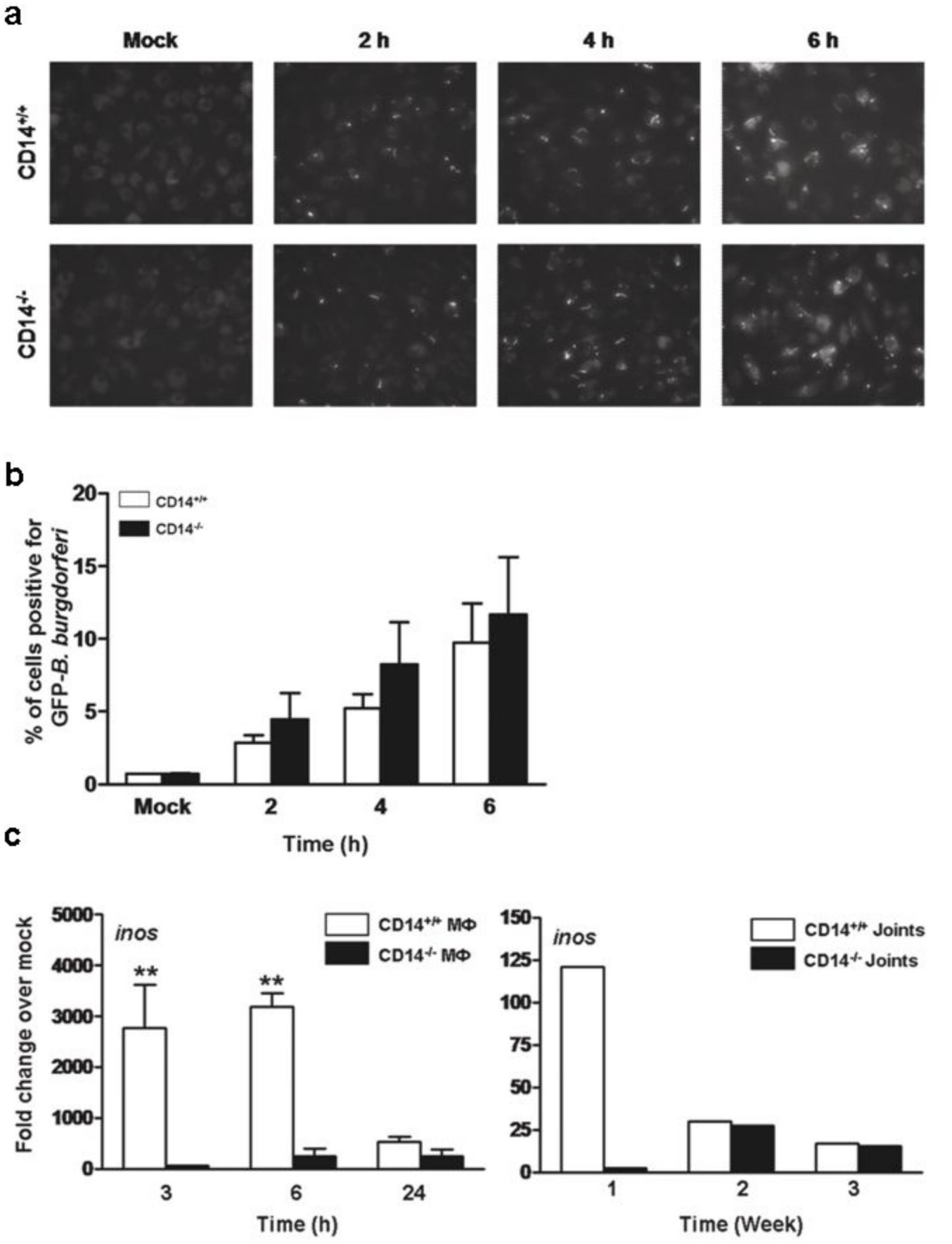
a
Mock
2 h
4 h
6 h
CD14+/+
CD14-/-
b
CD14+/+
CD14-/-
% of cells positive for GFP-B. burgdorferi
20
15
10
5
0
Mock
2
4
6
Time (h)
c
inos
CD14+/+ MΦ
CD14-/- MΦ
Fold change over mock
5000
4000
3000
2000
1000
0
**
**
3
6
24
Time (h)
inos
CD14+/+ Joints
CD14-/- Joints
150
125
100
75
50
25
0
1
2
3
Time (Week)

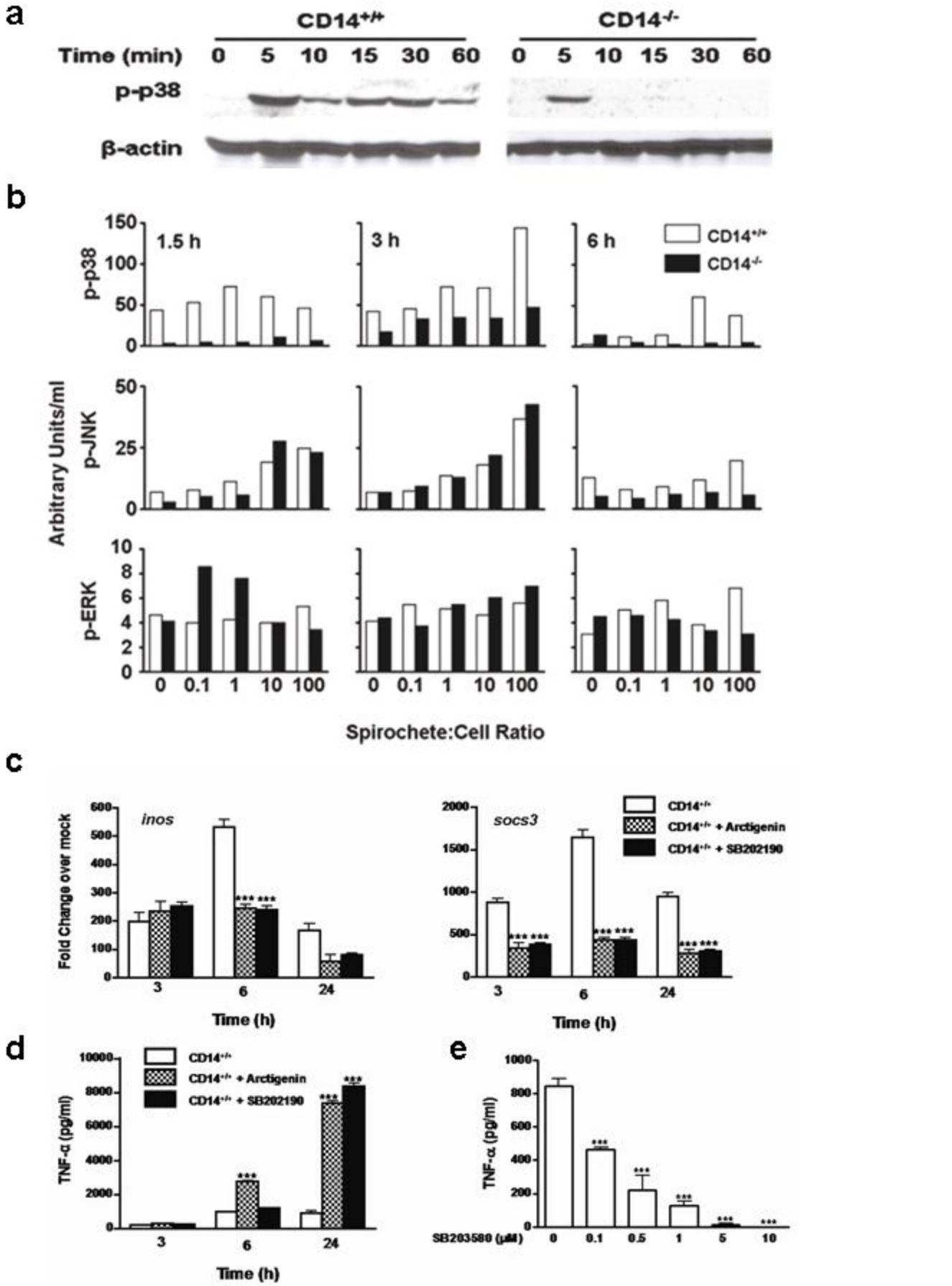
a
CD14+/+
CD14-/-
Time (min)
0 5 10 15 30 60
0 5 10 15 30 60
p-p38
β-actin
b
1.5 h
3 h
6 h
CD14+/+
CD14-/-
p-p38
p-JNK
p-ERK
Arbitrary Units/ml
0 0.1 1 10 100
Spirochete:Cell Ratio
c
inos
socs3
Fold Change over mock
CD14+/+
CD14+/+ + Arctigenin
CD14+/+ + SB202190
Time (h)
d
TNF-α (pg/ml)
e
SB203580 (μM)
0 0.1 0.5 1 5 10

a

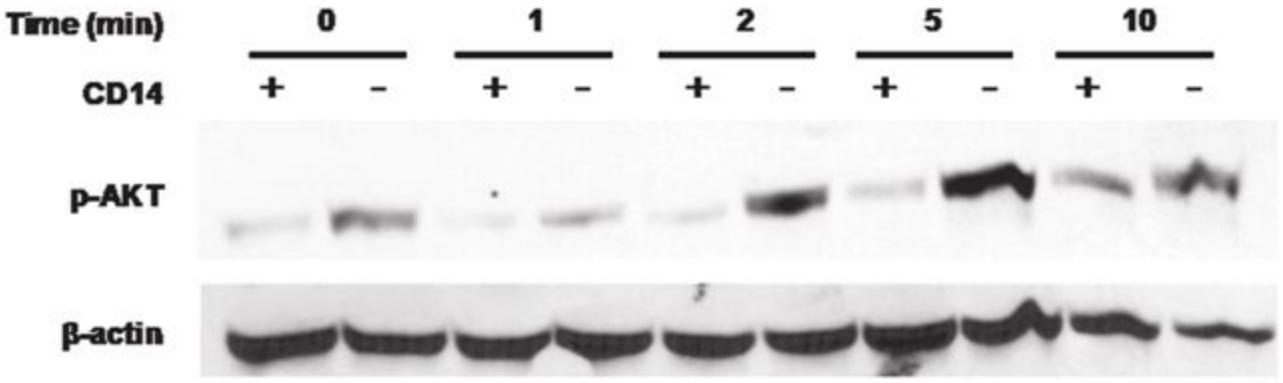
Time (min)
0
1
2
5
10
CD14
+ - + - + - + - + -
p-AKT
β-actin

b

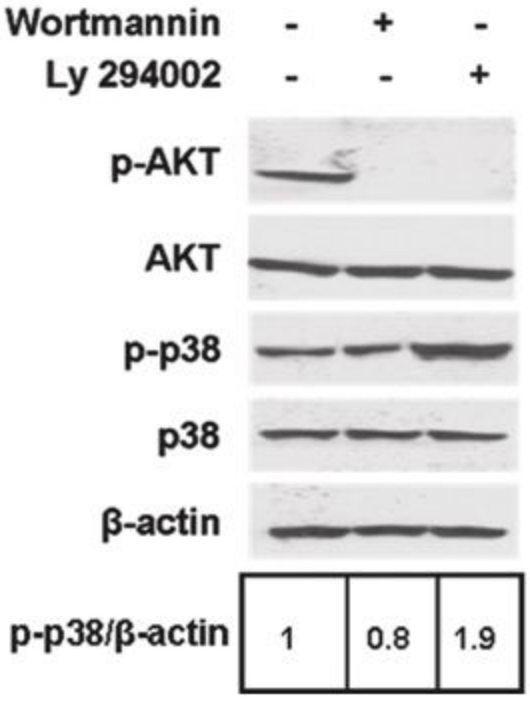
Wortmannin - + -
Ly 294002 - - +
p-AKT
AKT
p-p38
p38
β-actin
p-p38/β-actin
1
0.8
1.9

c

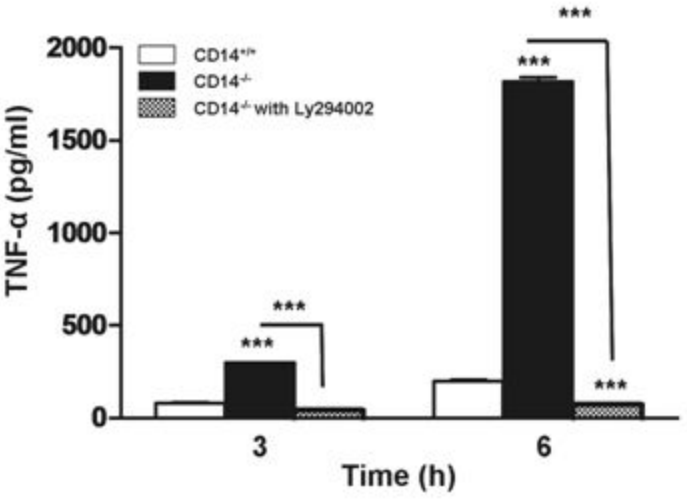
CD14+/+
CD14-/-
CD14-/- with Ly294002
TNF-α (pg/ml)
2000
1500
1000
500
0
***
***
***
***
***
3
6
Time (h)

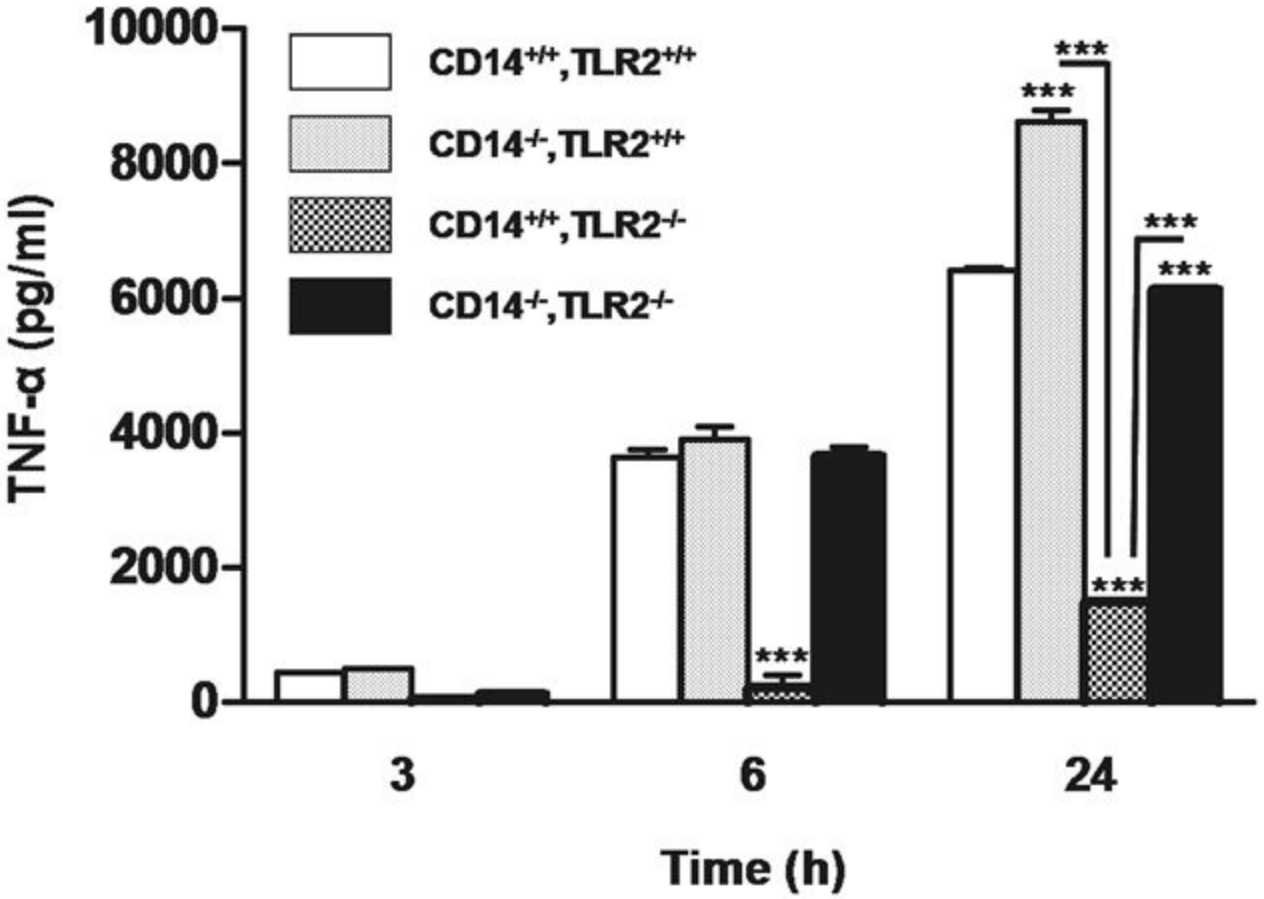
10000
8000
6000
4000
2000
0
TNF-α (pg/ml)
CD14+/+,TLR2+/+
CD14-/-,TLR2+/+
CD14+/+,TLR2-/-
CD14-/-,TLR2-/-
***
***
***
***
***
***
3
6
24
Time (h)

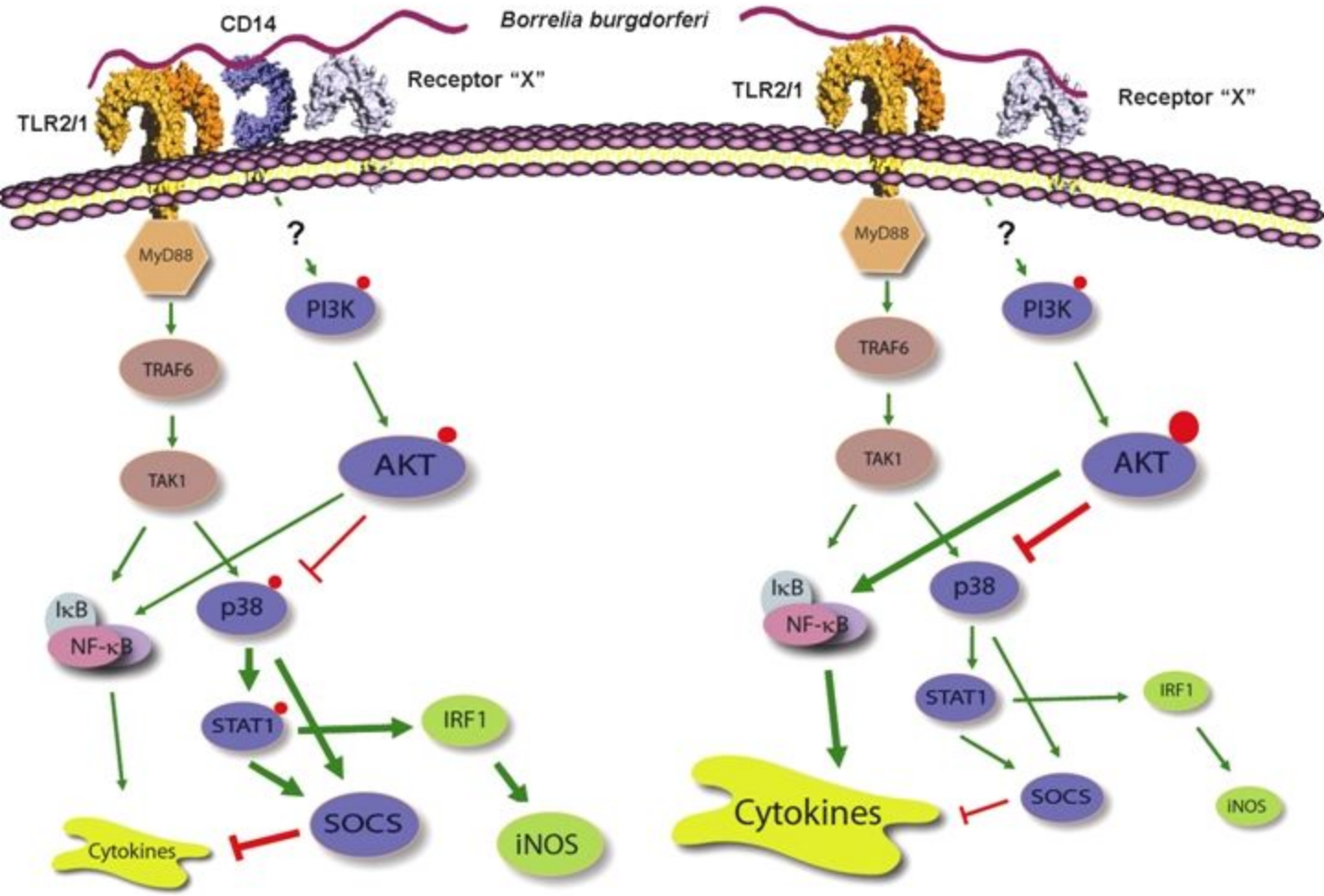
CD14
Borrelia burgdorferi
Receptor "X"
TLR2/1
MyD88
?
PI3K
TRAF6
TAK1
AKT
IκB
NF-κB
p38
STAT1
IRF1
SOCS
iNOS
Cytokines
TLR2/1
Receptor "X"
MyD88
?
PI3K
TRAF6
TAK1
AKT
IκB
NF-κB
p38
STAT1
IRF1
SOCS
iNOS
Cytokines